Unique insights into the intestinal absorption, transit, and subsequent biodistribution of polymer-derived microspheres

Joshua J. Reineke[a,1], Daniel Y. Cho[b,1], Yu-Ting Dingle[b], A. Peter Morello III[b], Jules Jacob[b], Christopher G. Thanos[b], and Edith Mathiowitz[b,2]

[a]Department of Pharmaceutical Sciences, Eugene Applebaum College of Pharmacy and Health Sciences, Wayne State University, Detroit, MI 48202; and [b]Department of Molecular Pharmacology, Physiology and Biotechnology, Brown University, Providence, RI 02912

Polymeric microspheres (MSs) have received attention for their potential to improve the delivery of drugs with poor oral bioavailability. Although MSs can be absorbed into the absorptive epithelium of the small intestine, little is known about the physiologic mechanisms that are responsible for their cellular trafficking. In these experiments, nonbiodegradable polystyrene MSs (diameter range: 500 nm to 5 μm) were delivered locally to the jejunum or ileum or by oral administration to young male rats. Following administration, MSs were taken up rapidly (≤5 min) by the small intestine and were detected by transmission electron microscopy and confocal laser scanning microscopy. Gel permeation chromatography confirmed that polymer was present in all tissue samples, including the brain. These results confirm that MSs (diameter range: 500 nm to 5 μm) were absorbed by the small intestine and distributed throughout the rat. After delivering MSs to the jejunum or ileum, high concentrations of polystyrene were detected in the liver, kidneys, and lungs. The pharmacologic inhibitors chlorpromazine, phorbol 12-myristate 13-acetate, and cytochalasin D caused a reduction in the total number of MSs absorbed in the jejunum and ileum, demonstrating that nonphagocytic processes (including endocytosis) direct the uptake of MSs in the small intestine. These results challenge the convention that phagocytic cells such as the microfold cells solely facilitate MS absorption in the small intestine.

oral delivery | uptake mechanism

Beginning in the 1960s, several groups (1–7) demonstrated that the small intestine could absorb microparticles with a diameter >1 μm, challenging dogma that the small intestine could only absorb small macromolecules. After this discovery, researchers began engineering microspheres (MSs) to deliver drugs with poor water solubility (8–10), poor gastrointestinal permeability (11), or poor oral bioavailability (8, 9, 12–15) to the small intestine. MS-based oral drug delivery systems (ODDSs) can be made from biodegradable polymers (12, 16–18), nondegradable polymers (19–21), and polysaccharides (22, 23) and can be engineered to carry polypeptides (18, 24, 25) and other molecules (26, 27). The motivation for using microparticulate-based ODDSs is to improve the oral bioavailability of drugs by enhancing their delivery and transit through the absorptive epithelium of the small intestine. This work may ultimately enable patients to take medications orally instead of relying on daily or weekly injections or other, less convenient routes of administration (28).

More than five decades after Sanders and Ashworth discovered that the small intestine can engulf large particles (1), little is known today about the cellular mechanisms or physiologic pathways that facilitate the absorption, transit, and biodistribution of microparticles that are delivered to the small intestine. Nonetheless, the diverse physiology and multitude of cell types in the small intestine likely play a central role in these processes. The absorptive epithelium is comprised primarily of enterocytes, cells that are critical for nutrient absorption (29–33). The distal jejunum and ileum contain a greater density of Peyer's patches and follicle-associated epithelium (FAE), regions that contain microfold (M) cells, which can facilitate the uptake of antigens (29, 34, 35), viruses (36, 37), and microorganisms (38, 39).

Given the immunological importance and phagocytic activity of M cells, researchers have focused on delivering microparticulate-based ODDSs to the Peyer's patches and the FAE (40, 41), both of which were once thought to be the regions chiefly responsible for microparticle uptake in the small intestine (42–47). However, non-FAE tissue can also play a role in the absorption and transit of MSs (48, 49). Despite the promise of M cell–targeted delivery, M cells comprise <1% of the total surface area of the absorptive epithelium; their scarcity makes targeting these cells difficult.

Many groups have used qualitative or semiquantitative methods to estimate the absorption and biodistribution of MSs in the small intestine, yet very few groups (50) have used quantitative methods to measure the actual percentage of MSs that are absorbed in the small intestine relative to the administered dose. Furthermore, very little research has been done in vivo to understand the specific cellular mechanisms that facilitate MS uptake, the relative importance of each mechanism, or the biodistribution of MSs following oral administration. Understanding the biodistribution and ultimate fate of MSs following ingestion are important for drug targeting, pharmacokinetics, and toxicology.

The objectives of our experiments were threefold: use electron and confocal microscopy to confirm the uptake of polystyrene MSs in the small intestine; approximate the number of polystyrene MSs that are absorbed in the small intestine; and determine the biodistribution of polystyrene MSs following oral or local delivery to the small intestine. In addition, we compared total uptake in the presence and absence of cellular inhibitors to determine which pathways facilitate MS uptake in the small intestine.

Results

Transmission Electron Microscopy. Ultrastructural analysis of the small intestine revealed that it was not damaged during the isolated loop surgical procedure. Five minutes after isolating the intestinal loop, MSs (200 nm) were detected in the intestinal lumen adjacent to the microvilli (brush border) of the absorptive epithelium (Fig. 1*A*). MSs (200 nm) were also observed within

APPLIED BIOLOGICAL SCIENCES

enterocytes (Fig. 1 *B* and *C*). After 5 min, larger MSs (500 nm) were observed within enterocytes near the lateral membrane of the apical cell boundary (Fig. 1*D*) and within cytosolic vesicles (Fig. 1*E*).

Confocal Microscopy. Fig. 2 shows representative confocal laser scanning micrographs (CLSMs) of rat jejunum (villus) after completion of a 1-h isolated loop procedure. In Fig. 2 *A* and *B*, the jejunum was observed after staining the tissue with DAPI and FM 1-43 stain. In Fig. 2*C*, fluorescent polystyrene MSs (500 nm) were observed within the jejunum. An overlay of Fig. 2 *A–C* revealed that MS traversed from the intestinal lumen through the apical membrane of enterocytes into the villus core (Fig. 2*D*). 3D fluorescence image analysis confirmed that MSs were colocalized within the tissue and were not separated from the intestine during specimen preparation.

Gel Permeation Chromatography. *Effect of microsphere diameter on absorption in the small intestine.* The uptake of polystyrene MSs following oral administration (fed) or local delivery to the jejunum or ileum is shown in Fig. 3. Total uptake was generally inversely related to MS diameter, independent of delivery method (local vs. oral), yet a greater percentage of 5-µm MSs was absorbed in the jejunum and ileum compared with 2-µm MSs. In the jejunum and ileum, 1- and 2-µm MSs were less likely to be absorbed than 500-nm MSs. A greater number of 500-nm MSs were absorbed in the jejunum compared with the ileum (45.8 ±

8.6% vs. 34.9 ± 9.3%, respectively). In the ileum, total uptake of 500-nm and 1-µm MSs was similar (34.9 ± 9.3% vs. 32.2 ± 11.5%, respectively). Following oral administration, uptake of 500-nm and 1-µm MSs was smaller compared with the uptake observed after delivery to the jejunum and ileum.

Microsphere biodistribution. Fig. 4*A* shows MS uptake following local administration to the jejunum (500 nm) and ileum (1 µm). One hour following the administration of 500-nm MSs, small concentrations of polymer were detected, but a greater concentration of polymer following the administration of 1-µm MSs was detected. After 3 h, greater quantities of 500-nm and 1-µm MSs were detected. After 5 h, a greater concentration of polymer was detected in animals that received 500-nm MSs compared with animals who received 1-µm MSs.

The concentration of polymer (expressed as a percentage of total uptake) following local delivery of 500-nm MSs to the jejunum is shown in Fig. 4*B*. After 1 h, the concentration of polymer detected in all assayed regions was low. After 3 h, a greater concentration of polymer was detected within the liver than all other regions combined. After 5 h, >30% of the total cumulative administered dose was detected within the liver, and a small but increasing concentration of polymer was detected within the kidneys.

The concentration of polymer (expressed as a percentage of total uptake) following local delivery of 1-µm MSs to the ileum is shown in Fig. 4*C*. One hour after local administration, more polymer was detected in the lungs than any other region; very
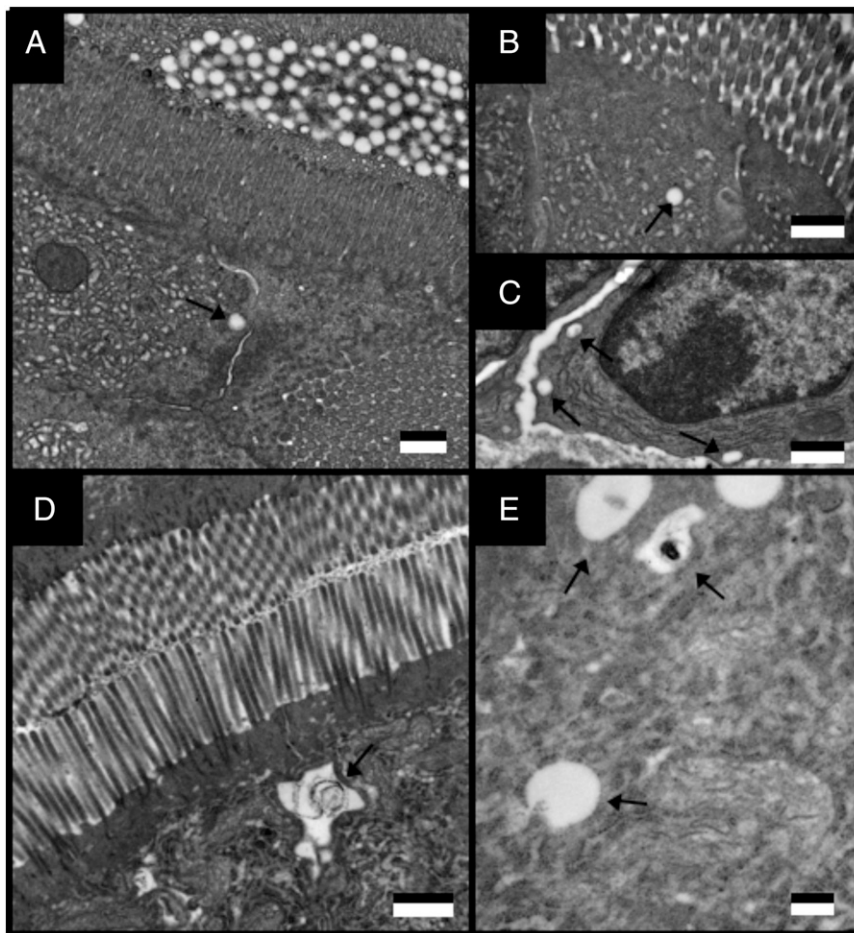

Fig. 1. TEM images of 200- (*A–C*) and 500-nm (*D* and *E*) polystyrene MSs 5 min after local delivery to the rat jejunum. Arrows indicate the location of MSs. (Scale bar, 500 nm.)
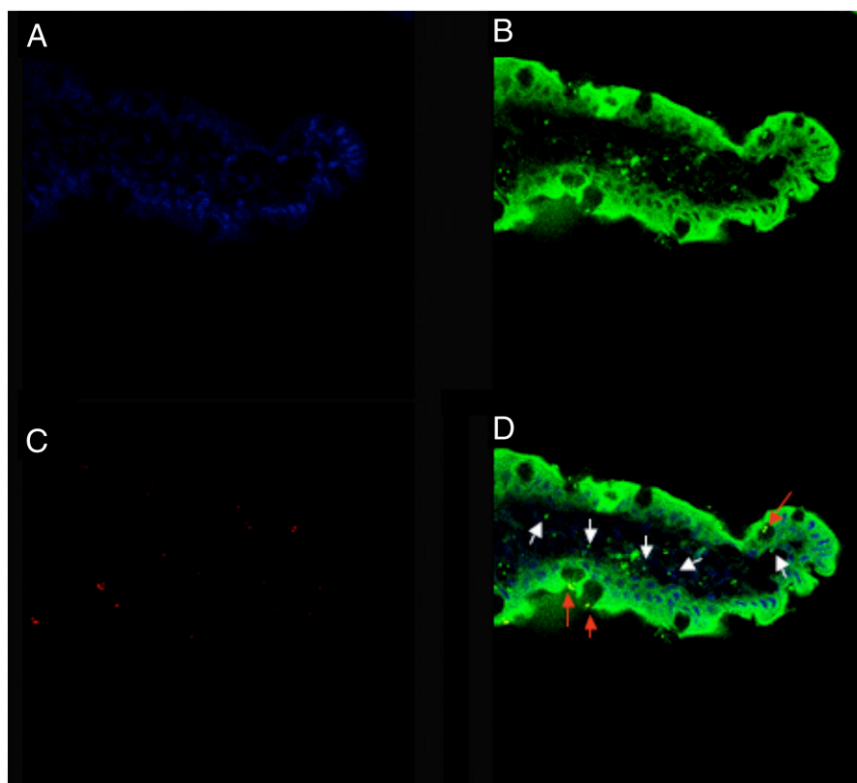
Reineke et al.

www.manaraa.com

Fig. 2. CLSM images of a single villus 1 h after delivering fluorescent PC-red 500-nm polystyrene MSs to the jejunum is shown with DAPI stain (*A*), FM 1-43 stain (*B*), and with illumination of fluorescent PC-red MSs (*C*). (*D*) Overlay of all three channels (*A–C*) is shown. In *D*, red arrows show where MSs are located within goblet cells; white arrows highlight where MS have penetrated beyond the epithelial cell layer.

little polymer was detected in the liver. After 3 h, smaller concentrations of polymer were found within the lungs, and more polymer was detected in the liver and kidneys. After 5 h, a higher concentration of polymer was detected in the liver, kidneys, and lungs compared with other assayed regions.

Fig. 4*D* shows the concentration of polymer following the oral administration of 500-nm and 1-μm MSs to rats. After 5 h, a greater number of 500-nm MSs were detected in the stomach relative to larger MSs, yet a greater number of 1-μm MSs were found within the jejunum, ileum, colon, and cecum (Fig. 4*D*). After 5 h, very few 500-nm and 1-μm MSs were found within the duodenum.

The biodistribution of MS following oral administration or local delivery to the jejunum or ileum is shown in Table S1. Five hours after administering 500-nm MSs, more polymer was detected in the liver than any other region. Larger MSs (1, 2, and 5 μm) were also detected in the liver, albeit in smaller quantities. Following local MS administration to the jejunum and ileum, a greater concentration of polymer was detected in the liver, kidneys, and lungs compared with other assayed regions. Polymer was detected in almost every tissue sample, including the brain.
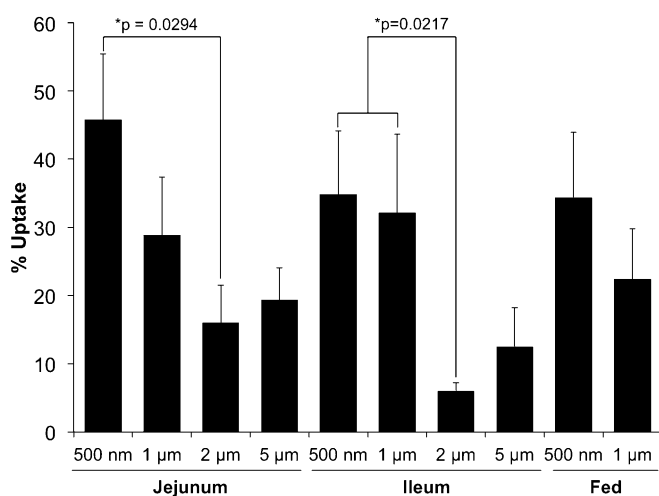
Effect of Endocytosis Inhibitors on Microsphere Uptake in the Jejunum and Ileum. Fig. 5 shows the total uptake of MS in the jejunum (Fig. 5*A*) and ileum (Fig. 5*B*) following local delivery of endocytosis blockers to these regions. After 5 h, the endocytosis blockers chlorpromazine (CPZ), phorbol 12-myristate 13-acetate (PMA), and cytochalasin D (CytD) caused a reduction in the total number of MSs absorbed by the jejunum relative to untreated animals ($3.6 \pm 2.1\%$, $10.3 \pm 2.3\%$, and $7.5 \pm 2.0\%$ for CPZ, PMA, and CytD, respectively, vs. $45.8 \pm 8.6\%$ for untreated animals). Five hours after administering the pharmacologic inhibitors to the ileum, MS uptake decreased relative to untreated animals ($12.1 \pm 3.6\%$, $14.4 \pm 3.6\%$, and $4.5 \pm 1.6\%$ for CPZ, colchicine, and CytB, respectively, vs. $32.2 \pm 11.5\%$ in the absence of inhibitor). In addition to observing a decrease in the quantity of MSs detected within each animal, the biodistribution of MSs was slightly changed relative to nontreated animals following administration of the endocytosis blockers (Fig. S1).

Fig. 3. Effect of polystyrene MS diameter on total uptake (expressed as a percentage of total administered dose) 5 h after local delivery to the jejunum or ileum or 5 h after oral administration. *n* = 4 animals for each cohort.
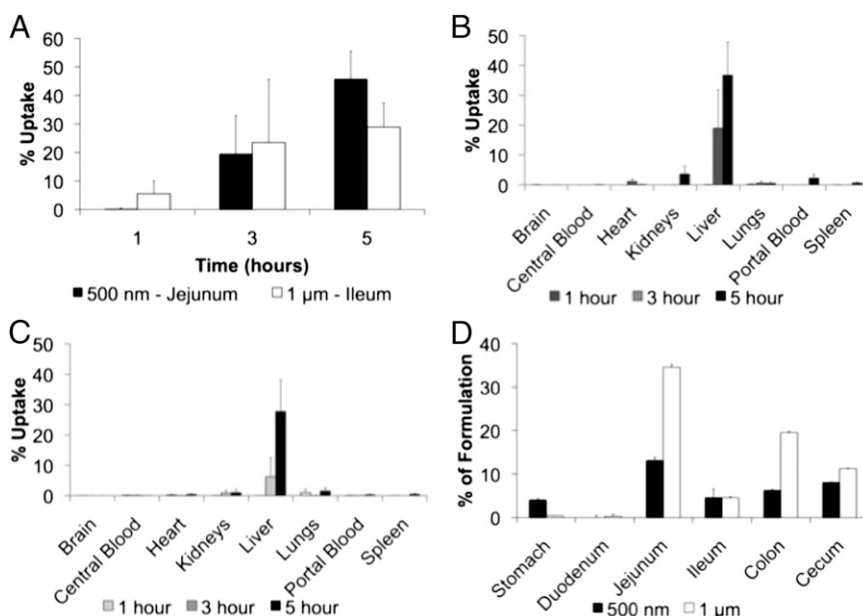
Reineke et al.

www.manaraa.com

Fig. 4. (*A*) Effect of time on the uptake of polystyrene microspheres in the jejunum and ileum is shown. The biodistribution of 500-nm MSs 1, 3, and 5 h after local delivery to the jejunum (*B*) and 1-μm MSs 1, 3, and 5 h after local delivery to the ileum (*C*) are also shown. *D* shows quantitative resident time analysis of 500-nm and 1-μm MSs 5 h after oral administration.

Discussion

The transport across the mucus layer is an important aspect in particle uptake. We have recently published a paper where the interaction of adhesive particles with the mucus is discussed in more detail (Fig. 1) (51). There are many factors involved in mucus transport that cannot be fully discussed here. For example, these particles are hydrophobic in nature, so there may be a hydrophobic driving force "pushing" particles toward the gut walls and away from the aqueous lumen. Regardless of the specific mechanisms involved in mucus transport, we feel that it occurs and the fact that orally fed particles (in absence of effects from the artificial isolated loop administration) also experience high uptake is strong evidence of this transport (51).

These experiments (Fig. 1) provide qualitative and quantitative confirmation that polystyrene MSs are taken up by the absorptive epithelium and deposited throughout the rat. Historically, there have been several proposed mechanisms for MS absorption, including endocytosis, which was believed to be limited to particles with a diameter <50 nm. In addition, paracellular transport of MSs between the tight junctions of enterocytes and phagocytosis by M cells were believed to facilitate MS uptake. Although a number of studies have provided evidence that enterocytes can engulf MSs in vitro and in vivo, non–Peyer's patch uptake by intestinal enterocytes is thought to be minimal. Furthermore, only one literature review in the last decade has recognized the importance of enterocytes and the absorptive epithelium in MS uptake. Delivery to enterocytes would be highly advantageous, especially given that M cells comprise a relatively small proportion of the small intestine's total surface area.

Data from these studies challenge current dogma in the area of oral drug delivery. Using an in vivo isolated loop technique for mechanistic studies has the advantage of isolating a specific intestinal region and being able to deliver specific pharmacologic uptake inhibitors locally in a controlled manner. In contrast, in vitro cell culture models are used to study the transepithelial transport of small molecule drugs. Several groups have used in vitro cell culture models to study the absorption of starch, polystyrene, poly(acrylic acid), and poly(lactic-coglycolic acid). Many of these studies have used Caco-2 cells derived from a

human colon adenocarcinoma cell line that differentiate into cells mimicking enterocytes. HT29 cells mimic goblet cells and incorporate a mucosal layer into the cell monolayers. Cocultures of Caco-2 and HT29 adenocarcinoma cells have been used to approximate the physiology of the small intestine, yet very few studies have looked at specific cellular mechanisms responsible for particle uptake. Furthermore, the predominant cell models (including Caco-2 cell monolayers) vary greatly in morphology, which may undergo even greater change in the presence of MS. Additionally, the relevance of an in vitro cell culture line to the dynamic in vivo environment (i.e., gastrointestinal mobility, fluid flow, mucus secretion, cell turnover) may not be suitable for studying the absorption, translocation, and biodistribution of MSs.

Transmission electron microscopy (TEM) in these studies revealed that 200- and 500-nm MSs were found within cytosolic vesicles. No exocytotic events were observed, which may be a result of the short duration of these experiments. We observed greater uptake of 500-nm polystyrene MSs in the absorptive epithelium of the jejunum than in the Peyer's patches of the ileum, indicating that an alternative mechanism to M cell phagocytosis facilitates MS uptake. Intestinal enterocytes are not capable of phagocytosis, which suggests that endocytosis facilitates MS uptake in the jejunum. Endocytosis of particles >1 μm has not been described in the literature, and only a single report by Rejman et al. noted that 500-nm MSs could be engulfed by endocytosis. Although the total uptake of 500-nm and 1-μm polystyrene MSs was lower relative to the total uptake observed following delivery of MSs locally to the jejunum and ileum, the uptake of MSs following oral delivery still comprised a relatively high proportion of the total administered dose.

In the jejunum and ileum, MS uptake steadily increased following MS administration, yet the manner in which they increased was slightly different. In the jejunum, MS uptake increased in a linear fashion, whereas in the ileum, MS uptake plateaued early in the study. One possible explanation for the lag time observed in the jejunum could be that more interaction time or intercellular signaling responses are required. In contrast, MS uptake in the ileum appeared to become saturated, leading to a plateau effect. Given these findings—and despite being the least studied
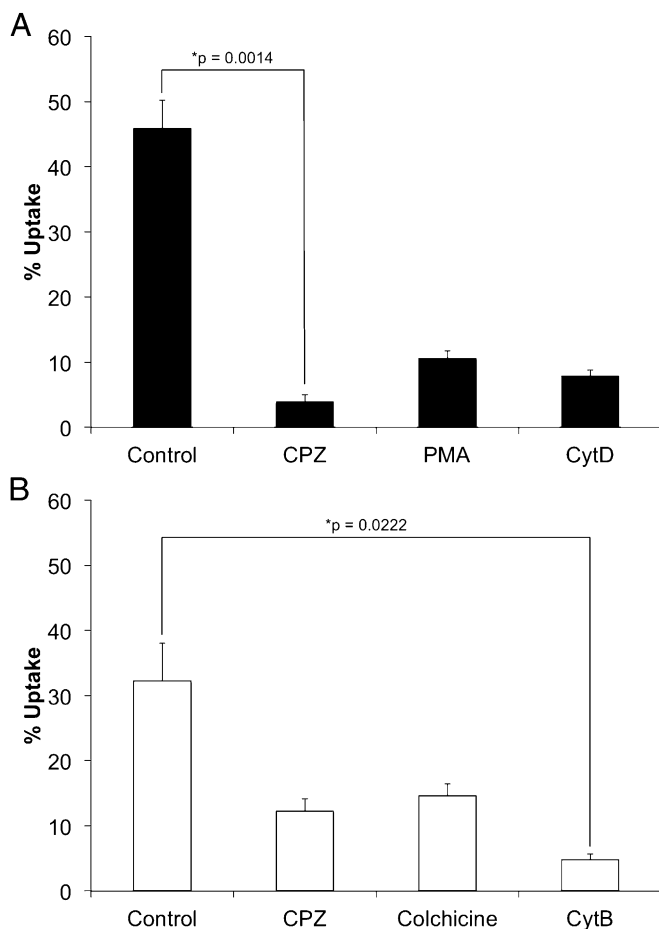
Reineke et al.

Fig. 5. (*A*) Total MS uptake is expressed as a percentage of the total administered dose following local delivery of 500-nm polystyrene MSs to the jejunum in the absence of drug (control) and with CPZ, PMA, and CytD. (*B*) Total MS uptake is expressed as a percentage of the total administered dose 5 h after local delivery of 1-μm polystyrene MSs to the ileum in the presence of CPZ, colchicine, and CytB and in the absence of drug.

mechanism—it is possible that a nonphagocytic mechanism in the jejunum is most responsible for MS uptake.

There are two known types of receptor-mediated endocytosis: clathrin dependent and clathrin independent. Our data suggest that the primary mechanism of MS uptake in the rat small intestine is via clathrin-mediated endocytosis in combination with caveolar-mediated endocytosis and phagocytosis. Clathrin-dependent endocytosis requires adaptor protein (AP) and a GTP-binding protein (dynamin) in addition to clathrin. AP2 facilitates membrane curvature and links the membrane proteins to clathrin, which is a three-limbed shaped protein that polymerizes to form cage-like structures. After transporting particles, clathrin must be recycled to form pits de novo; the binding site of AP2 must be inactivated to release clathrin (52, 53). CPZ activates the recycling AP2 binding sites that are normally inactive and causes the binding of AP2/clathrin. The inhibition of clathrin recycling prevents further endocytosis (53). Okamoto et al. showed that 25 μg/mL of CPZ inhibits clathrin-dependent endocytosis in Chinese hamster ovary cells (54).

Another well-known endocytotic pathway involves the formation of caveolae (cholesterol-rich membrane regions) that can easily invaginate due to a localized increase in membrane flexibility. Caveolae can bud off from the membrane, resulting in endocytosis of extracellular content. PMA exerts its effects through a protein kinase C–mediated mechanism, specifically through the phosphorylation of caveolin, a necessary protein in the formation of caveolae, to inhibit caveolin-mediated endocytosis without affecting the return of vesicles to the cell surface (55). Smart et al. showed an absence of folate uptake in M104 cells treated with PMA, specifically through the inhibition of a caveolin-mediated uptake mechanism (56). Similar results with micromolar concentrations of PMA have also been seen inhibiting virus entry into cells (57).

Although MSs were distributed throughout the rat, the majority of particles were found in the liver. Following MS delivery to the ileum, numerous MSs were spread among many organs, including the heart and spleen. This shift in organ distribution supports the theory that there may be different particle uptake mechanisms and distribution pathways. Peyer's patches are often referred to as gut-associated lymphoid tissue, or GALT, due to the fact that lymph nodes occupy the mucosal layer immediately beneath Peyer's patches. Increased MS distribution to the heart and spleen may be the result of MS traveling in the lymph, which passes through the lymphatic ducts and returns into the systemic circulation through the thoracic duct. Lymph does not undergo first pass metabolism, which may have allowed some of the MS to bypass the liver via lymphatic circulation. When MSs are delivered to the jejunum, distribution to the spleen and heart diminish due to an absence of FAE and Peyer's patches; these particles enter the hepatic circulation and are directed to the liver, which may lead to greater particle accumulation in the liver.

Conclusions

The uptake kinetics and biodistribution of polystyrene MSs following oral or local delivery to rat intestine was dependent on MS size, location, and route of administration. This study demonstrated that the nonlymphoid tissue of the absorptive epithelium can absorb MSs and facilitate their biodistribution throughout the rat. The relatively high degree of MS uptake in the absorptive and nonabsorptive epithelium indicates that endocytotic and phagocytotic mechanisms are responsible for MS uptake in the small intestine. These findings may potentially guide research aimed at delivering specific molecules to target organs. In addition, the methods and in vivo model used herein may also be useful to toxicologists who are interested in determining the fate or tissue distribution of microparticles, including whether such particles can cross the blood–brain barrier.

Materials and Methods

Polystyrene MSs with mean diameters of 500 nm and 1, 2, and 5 μm were purchased from Polysciences and administered both locally using an isolated loop procedure (with and without the addition of pharmacologic inhibitors CPZ, PMA, CytB and CytD, and colchicine) and by oral gavage. Total MS uptake following oral administration was quantified after 5 h. All animals were killed and had the following samples collected: portal vein blood (~1 mL), celiac arterial blood (~1 mL), lungs, heart, spleen, kidneys, liver, stomach, stomach rinse, duodenum, duodenum rinse, jejunum, jejunum rinse, ileum, ileum rinse, cecum, cecum rinse, colon, colon rinse, and brain. Gel permeation chromatography, TEM, and confocal microscopy were used to analyze the uptake of MS from collected tissues. For more details, see *SI Materials and Methods*.

1. Sanders E, Ashworth CT (1961) A study of particulate intestinal absorption and hepatocellular uptake. Use of polystyrene latex particles. *Exp Cell Res* 22:137–145.
2. Volkheimer G, Schulz FH (1968) The phenomenon of persorption. *Digestion* 1(4):213–218.
3. Volkheimer G (1974) Passage of particles through the wall of the gastrointestinal tract. *Environ Health Perspect* 9:215–225.
4. Alpar HO, Field WN, Hyde R, Lewis DA (1989) The transport of microspheres from the gastrointestinal tract to inflammatory air pouches in the rat. *J Pharm Pharmacol* 41(3):194–196.
5. Jani P, Halbert GW, Langridge J, Florence AT (1989) The uptake and translocation of latex nanospheres and microspheres after oral administration to rats. *J Pharm Pharmacol* 41(12):809–812.

Reineke et al.

6. LeFevre M, Boccio AM, Joel DD (1989) Intestinal uptake of fluorescent microspheres in young and aged mice. *Proceedings of the Society for Experimental Biology and Medicine* 190:23–27.

7. Pappo J, Ermak TH (1989) Uptake and translocation of fluorescent latex particles by rabbit Peyer's patch follicle epithelium: A quantitative model for M cell uptake. *Clin Exp Immunol* 76(1):144–148.

8. Thanos CG, et al. (2003) Enhancing the oral bioavailability of the poorly soluble drug dicumarol with a bioadhesive polymer. *J Pharm Sci* 92(8):1677–1689.

9. Thanos CG, Liu Z, Reineke J, Edwards E, Mathiowitz E (2003) Improving relative bioavailability of dicumarol by reducing particle size and adding the adhesive poly(fumaric-co-sebacic) anhydride. *Pharm Res* 20(7):1093–1100.

10. Wang J, et al. (2003) Release of paclitaxel from polylactide-co-glycolide (PLGA) microparticles and discs under irradiation. *J Microencapsul* 20(3):317–327.

11. Bhise SB, More AB, Malayandi R (2010) Formulation and in vitro evaluation of rifampicin loaded porous microspheres. *Sci Pharm* 78(2):291–302.

12. Wischke C, Schwendeman SP (2008) Principles of encapsulating hydrophobic drugs in PLA/PLGA microparticles. *Int J Pharm* 364(2):298–327.

13. Kwak HH, et al. (2009) Development of a sustained-release recombinant human growth hormone formulation. *J Controlled Release* 137(2):160–165.

14. Lanke SS, Gayakwad SG, Strom JG, D'souza MJ (2009) Oral delivery of low molecular weight heparin microspheres prepared using biodegradable polymer matrix system. *J Microencapsul* 26(6):493–500.

15. Khan F, Katara R, Ramteke S (2010) Enhancement of bioavailability of cefpodoxime proxetil using different polymeric microparticles. *AAPS PharmSciTech* 11(3):1368–1375.

16. Mathiowitz E, et al. (1997) Biologically erodable microspheres as potential oral drug delivery systems. *Nature* 386(6623):410–414.

17. Mundargi RC, Babu VR, Rangaswamy V, Patel P, Aminabhavi TM (2008) Nano/micro technologies for delivering macromolecular therapeutics using poly(D,L-lactide-co-glycolide) and its derivatives. *J Controlled Release* 125(3):193–209.

18. Pai SS, Tilton RD, Przybycien TM (2009) Poly(ethylene glycol)-modified proteins: Implications for poly(lactide-co-glycolide)-based microsphere delivery. *AAPS J* 11(1):88–98.

19. Ma GH, Nagai M, Omi S (1999) Effect of lauryl alcohol on morphology of uniform polystyrene-poly(methyl methacrylate) composite microspheres prepared by porous glass membrane emulsification technique. *J Colloid Interface Sci* 219(1):110–128.

20. Supsakulchai A, Ma GH, Nagai M, Omi S (2003) Preparation of uniform titanium dioxide (TiO2) polystyrene-based composite particles using the glass membrane emulsification process with a subsequent suspension polymerization. *J Microencapsul* 20(1):1–18.

21. Morello AP, 3rd, Burrill R, Mathiowitz E (2007) Preparation and characterization of poly(methyl methacrylate) - iron (III) oxide microparticles using a modified solvent evaporation method. *J Microencapsul* 24(5):476–491.

22. Varshosaz J (2007) The promise of chitosan microspheres in drug delivery systems. *Expert Opin Drug Deliv* 4(3):263–273.

23. Masotti A, Ortaggi G (2009) Chitosan micro- and nanospheres: Fabrication and applications for drug and DNA delivery. *Mini Rev Med Chem* 9(4):463–469.

24. Crotts G, Park TG (1998) Protein delivery from poly(lactic-co-glycolic acid) biodegradable microspheres: Release kinetics and stability issues. *J Microencapsul* 15(6):699–713.

25. Wu F, Jin T (2008) Polymer-based sustained-release dosage forms for protein drugs, challenges, and recent advances. *AAPS PharmSciTech* 9(4):1218–1229.

26. Pouponneau P, Leroux JC, Martel S (2009) Magnetic nanoparticles encapsulated into biodegradable microparticles steered with an upgraded magnetic resonance imaging system for tumor chemoembolization. *Biomaterials* 30(31):6327–6332.

27. Wang Y, et al. (2012) Synthesis of monodisperse, hierarchically mesoporous, silica microspheres embedded with magnetic nanoparticles. *ACS Appl Mater Interfaces* 4(5):2735–2742.

28. Akhtar S (2009) Oral delivery of siRNA and antisense oligonucleotides. *J Drug Target* 17(7):491–495.

29. Kyd JM, Cripps AW (2008) Functional differences between M cells and enterocytes in sampling luminal antigens. *Vaccine* 26(49):6221–6224.

30. Danielsen EM, Hansen GH (2008) Lipid raft organization and function in the small intestinal brush border. *J Physiol Biochem* 64(4):377–382.

31. Johansson ME, et al. (2011) Composition and functional role of the mucus layers in the intestine. *Cell Mol Life Sci* 68(22):3635–3641.

32. Mellitzer G, Gradwohl G (2011) Enteroendocrine cells and lipid absorption. *Curr Opin Lipidol* 22(3):171–175.

33. Miron N, Cristea V (2012) Enterocytes: Active cells in tolerance to food and microbial antigens in the gut. *Clin Exp Immunol* 167(3):405–412.

34. Bockman DE, Cooper MD (1973) Pinocytosis by epithelium associated with lymphoid follicles in the bursa of Fabricius, appendix, and Peyer's patches. An electron microscopic study. *Am J Anat* 136(4):455–477.

35. Owen RL (1977) Sequential uptake of horseradish peroxidase by lymphoid follicle epithelium of Peyer's patches in the normal unobstructed mouse intestine: An ultrastructural study. *Gastroenterology* 72(3):440–451.

36. Amerongen HM, et al. (1991) Transepithelial transport of HIV-1 by intestinal M cells: A mechanism for transmission of AIDS. *J Acquir Immune Defic Syndr* 4(8):760–765.

37. Lapenta C, et al. (1999) Human intestinal lamina propria lymphocytes are naturally permissive to HIV-1 infection. *Eur J Immunol* 29(4):1202–1208.

38. Owen RL, Pierce NF, Apple RT, Cray WC, Jr. (1986) M cell transport of Vibrio cholerae from the intestinal lumen into Peyer's patches: A mechanism for antigen sampling and for microbial transepithelial migration. *J Infect Dis* 153(6):1108–1118.

39. Wolf JL, et al. (1981) Intestinal M cells: A pathway for entry of reovirus into the host. *Science* 212(4493):471–472.

40. Clark MA, Jepson MA, Hirst BH (2001) Exploiting M cells for drug and vaccine delivery. *Adv Drug Deliv Rev* 50(1-2):81–106.

41. Kuolee R, Chen W (2008) M cell-targeted delivery of vaccines and therapeutics. *Expert Opin Drug Deliv* 5(6):693–702.

42. LeFevre ME, Hancock DC, Joel DD (1980) Intestinal barrier to large particulates in mice. *J Toxicol Environ Health* 6(4):691–704.

43. LeFevre ME, Boccio AM, Joel DD (1989) Intestinal uptake of fluorescent microspheres in young and aged mice. *Proceedings of the Society for Experimental Biology and Medicine* 190(1):23-27.

44. Simon L, Shine G, Dayan AD (1994) Effect of animal age on the uptake of large particulates across the epithelium of the rat small intestine. *Int J Exp Pathol* 75(5):369–373.

45. Hodges GM, Carr EA, Hazzard RA, Carr KE (1995) Uptake and translocation of microparticles in small intestine. Morphology and quantification of particle distribution. *Dig Dis Sci* 40(5):967–975.

46. Desai MP, Labhasetwar V, Amidon GL, Levy RJ (1996) Gastrointestinal uptake of biodegradable microparticles: Effect of particle size. *Pharm Res* 13(12):1838–1845.

47. Khan J, et al. (1997) Total parenteral nutrition increases uptake of latex beads by Peyer's patches. *JPEN J Parenter Enteral Nutr* 21(1):31–35.

48. Smyth SH, Feldhaus S, Schumacher U, Carr KE (2008) Uptake of inert microparticles in normal and immune deficient mice. *Int J Pharm* 346(1-2):109–118.

49. Carr KE, Smyth SH, McCullough MT, Morris JF, Moyes SM (2012) Morphological aspects of interactions between microparticles and mammalian cells: Intestinal uptake and onward movement. *Prog Histochem Cytochem* 46(4):185–252.

50. Jani P, Halbert GW, Langridge J, Florence AT (1990) Nanoparticle uptake by the rat gastrointestinal mucosa: Quantitation and particle size dependency. *J Pharm Pharmacol* 42(12):821–826.

51. Reineke J, et al. (2013) Can bioadhesive nanoparticles allow for more effective particle uptake from the small intestine? *J Control Release* 190(3):477–484.

52. Wang LH, Rothberg KG, Anderson RG (1993) Mis-assembly of clathrin lattices on endosomes reveals a regulatory switch for coated pit formation. *J Cell Biol* 123(5):1107–1117.

53. Atwood WJ (2001) A combination of low-dose chlorpromazine and neutralizing antibodies inhibits the spread of JC virus (JCV) in a tissue culture model: Implications for prophylactic and therapeutic treatment of progressive multifocal leukencephalopathy. *J Neurovirol* 7(4):307–310.

54. Okamoto Y, Ninomiya H, Miwa S, Masaki T (2000) Cholesterol oxidation switches the internalization pathway of endothelin receptor type A from caveolae to clathrin-coated pits in Chinese hamster ovary cells. *J Biol Chem* 275(9):6439–6446.

55. Parton RG, Joggerst B, Simons K (1994) Regulated internalization of caveolae. *J Cell Biol* 127(5):1199–1215.

56. Smart EJ, Foster DC, Ying YS, Kamen BA, Anderson RG (1994) Protein kinase C activators inhibit receptor-mediated potocytosis by preventing internalization of caveolae. *J Cell Biol* 124(3):307–313.

57. Empig CJ, Goldsmith MA (2002) Association of the caveola vesicular system with cellular entry by filoviruses. *J Virol* 76(10):5266–5270.

www.manaraa.com